Program Digest, 2019 IEEE International Ultrasonics Symposium (IUS)
Glasgow, Scotland, October 6-9, 2019

Maximum-Likelihood Estimation to Assess the Degree of Reconstruction of Microvasculature from Super-Resolution US Imaging

Stefanie Dencks
Institute for Medical Engineering
Ruhr-Universität Bochum
Bochum, Germany
stefanie.dencks@rub.de

Marion Piepenbrock
Institute for Medical Engineering
Ruhr-Universität Bochum
Bochum, Germany
marion.piepenbrock@rub.de

Georg Schmitz
Institute for Medical Engineering
Ruhr-Universität Bochum
Bochum, Germany
georg.schmitz@rub.de

***Abstract*—In clinical applications of super-resolution ultrasound imaging, the complete reconstruction of the microvasculature will not be feasible due to several limiting factors such as measurement times, concentrations of microbubbles, or motion artefacts. Therefore, it is of interest to estimate the degree of reconstruction in order to establish reasonable measurement protocols and to derive meaningful morphological and perfusion parameters. Here, we show that the filling of the voxels with the detected microbubbles (i.e. the reconstruction), can be well modeled with a zero-inflated Poisson (ZIP) process. For the first time – to our knowledge – we derived a closed-form solution for the maximum likelihood estimator (MLE) of the relevant parameters of a ZIP process. From these parameters, the degree of reconstruction can be assessed from the ratio of the number of filled voxels to the number of voxels that are expected to be filled after infinite time.**

We show, that in preclinical and clinical measurements a degree of reconstruction between 38% and 74% was achieved. We also demonstrate that reliable estimates can be achieved earlier with the MLE than with the least-squares fit to the data as previously proposed. Additionally, the MLE is very easy to implement as the counts observed at the end of the measurement period provide all necessary data for parameter estimation.

Keywords—closed-form, maximum-likelihood estimator, measurement times, saturation model, ultrasound localization microscopy, zero-inflated Poisson process

I. Introduction

The main interest in super-resolution imaging based on ultrasound localization microscopy (ULM) lies in the reconstruction of the microvasculature to analyze its morphological properties and to visualize and characterize the perfusion of relevant tissues. However, in clinical applications it will not be possible to reconstruct the complete microvasculature because of e.g. limited measurement times, restricted concentrations of microbubbles (MB), or motion artefacts.

To define and derive relevant and meaningful parameters in clinical applications, the degree of reconstruction of the microvasculature after limited measurement times is important for normalization. Recently, we showed that the percentage of reconstruction can be assessed based on an exponential saturation model and a corresponding least-squares fit (LSF) to the binary filling of the pixels over time [1, 2]. Here, we present an extended statistical model and a closed-form maximum likelihood estimator for the vascular filling problem, which has lower variance and allows to estimate the reconstruction degree from the final count map without the need of observations over time.

II. Theory

A. Statistical Model for ULM Count Maps

Super-resolved count maps are usually built by counting in each voxel the number of MB that have passed during the measurement time [3, 4]. Then, the number of counts k are encoded in different colors (see Fig. 1).

Counting processes of independent events at a constant rate are typically modeled with a Poisson distribution. Correspondingly, in voxels that belong to a vessel the probability for a certain number of passed MB can be modeled by

$$P_C\{X(t) = k\} = \frac{\Lambda^k}{k!} e^{-\Lambda}, \qquad \Lambda = \lambda t \tag{1}$$

where $X(t)$ is the number of passed MB, k the number of counts, λ the expected number of counts per voxel, and t the measurement time.

However, for an empty voxel without counts it is unknown whether just no MB passed by or whether this voxel does not contain a vessel (indicated by the question mark in Fig. 1).

We model the probability that a voxel contains a vessel by P_v. After infinite time the ratio of filled voxels to the total number of voxels would approach this value, which thus can also be used to measure the clinically relevant parameter *relative blood volume* (rBV). Then, the probability of showing no counts ($k = 0$) is the sum of the probability of a vessel voxel with no counts $P_v \cdot P_C\{X(t) = 0\}$ and the probability of an empty voxel $1 - P_v$. This results in more frequent zero-valued observations than predicted with a standard Poisson distribution and is modelled by the so-called zero-inflated Poisson (ZIP) distribution [5]:

(a) (b)

Fig. 1. Illustration of a count map of a super-resolved US image. (a) Original counts in a count map. The question mark visualizes the unknowingness whether just no microbubble passed or whether the voxel does not belong to a vessel. (b) Binarized version of the count map.

$$P\{X(t) = k\} = \begin{cases} (1 - P_v) + P_v e^{-\Lambda} & \text{for} \quad k = 0 \\ P_v \dfrac{\Lambda^k}{k!} e^{-\Lambda} & \text{for} \quad k > 0 \end{cases}. \tag{2}$$

The filling of the whole image with N voxels is modeled as the compound distribution of a vector-valued stochastic process $\boldsymbol{X}(t) = \big(X_1(t), \dots, X_N(t)\big)^T$. Using the sign function

$$\operatorname{sgn}(k) = \begin{cases} 1 & \text{for} \quad k > 0 \\ 0 & \text{for} \quad k = 0 \end{cases} \tag{3}$$

and assuming stochastically independent and identically distributed voxels the joint probability mass function to observe the count vector $\boldsymbol{k} = (k_1, \dots, k_N)^T$ is

$$P\{\boldsymbol{X} = \boldsymbol{k}\} = \prod_{n=1}^{N} \Big(1 - P_v(1 - e^{-\Lambda})\Big)^{1-\operatorname{sgn}(k_n)} \times \left(P_v \frac{\Lambda^{k_n}}{k_n!} e^{-\Lambda}\right)^{\operatorname{sgn}(k_n)}. \tag{4}$$

B. Maximum Likelihood Estimator

For this probability, the Maximum Likelihood Estimator (MLE) can be deduced by partially deriving the log-likelihood $\ln P\{\boldsymbol{X} = \boldsymbol{k}\}$ with respect to P_v and Λ and equalizing it to zero. This results in

$$\hat{\Lambda} = W_0\left(-\frac{T_2}{T_1} e^{-\frac{T_2}{T_1}}\right) + \frac{T_2}{T_1}, \tag{5}$$

with W_0 being the main branch of the Lambert's W-function and

$$\hat{P}_v = \frac{T_1}{N\big(1 - e^{-\hat{\Lambda}}\big)} = \frac{T_2}{N\hat{\Lambda}}, \tag{6}$$

where

$$T_1(\boldsymbol{X}) = \sum_{n=1}^{N} \operatorname{sgn}(X_n), \tag{7}$$

and

$$T_2(\boldsymbol{X}) = \sum_{n=1}^{N} X_n. \tag{8}$$

T_2 corresponds to the sum of all counts in the image (see Fig. 1 a) for the measurement time t. T_1 correspond to the number of filled voxels, i.e. the sum over the binarized count map (see Fig. 1 b). The Lambert's W-function is e.g. implemented in Matlab as lambertw (Mathworks, Natick, MA, USA).

In contrast to other formulations [6], this is a closed-form derivation of the MLE for a ZIP process.

C. Degree of Reconstruction

The degree of reconstruction DOR can be directly assessed with

$$\text{DOR} = \frac{T_1/N}{\hat{P}_v} = 1 - e^{-\hat{\Lambda}}. \tag{9}$$

III. Experimental Validation

The experimental validation was carried out with data from preclinical and clinical measurements that were acquired for earlier studies [7, 8].

A. Preclinical Data

All animal experiments were approved by the governmental animal care and use committee (LANUV).

The data of murine xenograft tumors (A431, A549, and MLS) were acquired using a Vevo 2100 system (FUJIFILM Visualsonics, Toronto, ON, Canada; MS-550D transducer, 40 MHz center frequency) during the destruction-replenishment sequence. The MB were fabricated with polybutyl-cyanoacrylate (PBCA) [9]. The frames were recorded with a frame rate of 50 Hz.

After a rigid motion compensation, the MB were localized in the B-mode images. MB (foreground) and tissue (background) were separated using a rank filter. The positions of the MB were computed by calculating the intensity weighted centroid [7]. The tracking of the MB was carried out with the Markov Chain Monte Carlo Data Association (MCMCDA) algorithm. Details of the tracking algorithm can be found in [10].

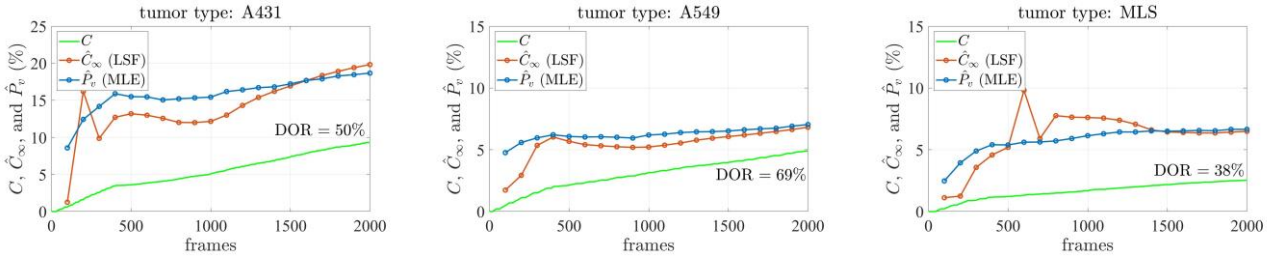

(a) (b) (c)

Fig. 2. Coverage C, final coverage $\hat{C}_\infty$ estimated with the LSF, and vessel probability $\hat{P}_v$ estimated with the MLE for increasing measurement times for exemplary murine xenograft tumors of type A431 (a), A549 (b), and MLS (c).

B. Clinical Data

The clinical study was approved by the RWTH Aachen University ethics committee and registered at clinicaltrials.gov under the number: NCT03385200. Written informed consent was obtained from all patients.

The clinical data of a triple negative breast carcinoma were acquired with an Aplio 500 (Canon Medical Systems, Otaware, Japan; PLT 1005BT transducer, 10 MHz center frequency) after injecting SonoVue (Bracco, Milan, Italy). The frames were recorded at a frame rate of 15 Hz [8].

Because the MB were not visible in the B-mode images they were localized in the contrast mode sequences. These were convolved in 2D with a Gaussian kernel matching the size of the point spread function of the MB. Then, the local intensity maxima were detected. These positions were corrected by the motion estimated in the B-mode images [8]. The tracking of the MB was also carried out with the MCMCDA algorithm.

C. Count Maps, Coverage, and Degree of Reconstruction

By accumulating the positions of the tracks in image matrices, count maps are computed. For the preclinical data, the grid size was 5 µm, for the preclinical data 10 µm [7]. Generally, for the ZIP model the pixel sizes should not become much larger than the smaller vessel sizes. Then, P_v can be used to model the rBV.

The ratio of T_1 to the total number of pixels N within the ROI is called *coverage* C. It is computed for increasing measurement times in steps of 50 frames. The *coverage* of the full reconstruction of the vasculature is expected to be related to the rBV as discussed above.

The final *coverage* estimated with the previously proposed LSF is named $\hat{C}_\infty$ [1, 2]. The equivalent vessel probability estimated with the proposed MLE is named $\hat{P}_v$. The degree of reconstruction DOR at the end of the measurement time is calculated by Eq. (9).

IV. Results

In Fig. 2, the results of exemplary preclinical data that visualize the main findings are shown. Generally, at the end of the measurement time, the $\hat{C}_\infty$ (red line) and $\hat{P}_v$ (blue line) estimated with the LSF and with the MLE, respectively, approach each other. It can also be seen, that a certain number of counts and thus a certain measurement time is necessary to get reliable results: At the beginning of the measurements (for very few counts) the estimated values are always too low. Nevertheless, P_v can be earlier reliably estimated. By trend, the differences between the estimations of $\hat{C}_\infty$ and $\hat{P}_v$ are smaller for low rBV. In Fig. 3, again data of a preclinical measurement is shown to illustrate that the estimation of $\hat{C}_\infty$ can also completely miss the mark. This effect was only observed for the application of the LSF. Also, in Fig. 4 showing clinical data the better performance of the MLE is clearly visible. Generally, the MLE yields more stable estimates.

After 40 s (preclinical measurement) or about 90 s (clinical measurements), a degree of reconstruction DOR of 38% to 74% was achieved.

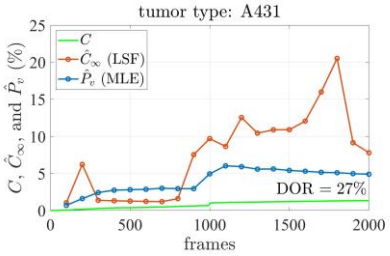

Fig. 3. Additional example for coverage C, final coverage $\hat{C}_\infty$ (LSF), and vessel probability $\hat{P}_v$ (MLE) that was excluded from further evaluations because of an artefact at frame 1000.

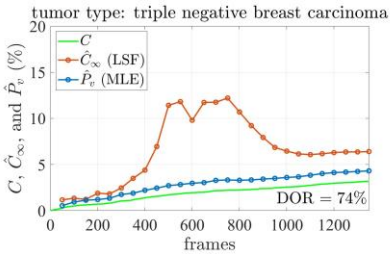

Fig. 4. Coverage C, final coverage $\hat{C}_\infty$ estimated with the LSF, and vessel probability $\hat{P}_v$ estimated with the MLE for increasing measurement times for triple negative breast carcinoma (example).

V. Discussion and Conclusion

By modeling the filling of count maps based on a zero-inflated Poisson process, a closed-form MLE was derived to assess the degree of reconstruction of the microvasculature in super-resolution imaging. On preclinical and clinical data, we showed that after feasible measurement times the degree of reconstruction can be very different. This makes it clear that the assessment of the DOR is essential for the correct interpretation of morphological and perfusion parameters that are derived from super-resolved US images and for the specification of measurement protocols. We also showed that the MLE outperforms the LSF method because it approaches stable estimates earlier. Furthermore, the derived closed-form MLE is very easy to implement and computationally efficient as all information is contained in the final count map without the need of evaluating the filling over time.

References

[1] S. Dencks, M. Piepenbrock, G. Schmitz, T. Opacic, and F. Kiessling, "Determination of adequate measurement times for super-resolution characterization of tumor vascularization," in *Proc. IEEE International Ultrasonics Symposium (IUS)*, 2017, pp. 1-4.

[2] S. Dencks, M. Piepenbrock, T. Opacic, B. Krauspe, E. Stickeler, F. Kiessling, *et al.*, "Relative blood volume estimation from clinical super-resolution us imaging in breast cancer," in *Proc. IEEE International Ultrasonics Symposium (IUS)*, 2018, pp. 1-4.

[3] K. Christensen-Jeffries, R. J. Browning, M.-X. Tang, C. Dunsby, and R. J. Eckersley, "In vivo acoustic super-resolution and super-resolved velocity mapping using microbubbles," *IEEE Transactions on Medical Imaging,* vol. 34, pp. 433-440, 2015.

[4] C. Errico, J. Pierre, S. Pezet, Y. Desailly, Z. Lenkei, O. Couture, *et al.*, "Ultrafast ultrasound localization microscopy for deep super-resolution vascular imaging," *Nature,* vol. 527, pp. 499-502, 2015.

[5] D. Lambert, "Zero-inflated poisson regression, with an application to defects in manufacturing," *Technometrics,* vol. 34, pp. 1-14, 1992.

[6] S. Beckett, J. Jee, T. Ncube, S. Pompilus, Q. Washington, A. Singh, *et al.*, "Zero-inflated poisson (zip) distribution: Parameter estimation and applications to model data from natural calamities," *Involve, a Journal of Mathematics,* vol. 7, pp. 751-767, 2014.

[7] T. Opacic, S. Dencks, B. Theek, M. Piepenbrock, D. Ackermann, A. Rix, *et al.*, "Motion model ultrasound localization microscopy for preclinical and clinical multiparametric tumor characterization," *Nature Communications,* vol. 9, 2018.

[8] S. Dencks, M. Piepenbrock, T. Opacic, B. Krauspe, E. Stickeler, F. Kiessling, *et al.*, "Clinical pilot application of super-resolution us imaging in breast cancer," *IEEE Transactions on Ultrasonics, Ferroelectrics, and Frequency Control,* vol. 66, pp. 517-526, 2019.

[9] S. Fokong, M. Siepmann, Z. Liu, G. Schmitz, F. Kiessling, and J. Gätjens, "Advanced characterization and refinement of poly n-butyl cyanoacrylate microbubbles for ultrasound imaging," *Ultrasound in Medicine & Biology,* vol. 37, pp. 1622-1634, 2011.

[10] D. Ackermann and G. Schmitz, "Detection and tracking of multiple microbubbles in ultrasound b-mode images," *IEEE Transactions on Ultrasonics, Ferroelectrics, and Frequency Control,* vol. 63, pp. 72-82, 2016.